Journal of the Physical Society of Japan
Vol. 62, No. 3, March, 1993, pp. 911–917

Polarization Interferometry of X-Ray Diffraction

Kouhei OKITSU

Department of Physics, Toyama University, Toyama 930

(Received March 4, 1992)

A new type of X-ray diffraction interferometry is described, in which σ- and π-polarized X-rays diffracted by a sample crystal interfere with each other. A reversal of image contrast in 'polarization interference topograph' due to contrary sign of a spherical strain field in a crystal is demonstrated in terms of numerical simulations by Takagi-Taupin's dynamical theory. Further, a feasibility of 'polarization holography' of X-ray diffraction is pointed out.

§1. Introduction

Polarization phenomena in X-ray dynamical diffraction have provided several interesting problems for scientists in this field. Polarization effects on Pendellösung fringes in X-ray diffraction topography were investigated by Hattori *et al.*[1] for the case of an unpolarized incident wave, and by Hart and Lang[2] for the cases of unpolarized and σ-polarized incident waves. Skalicky and Malgrange[3] investigated the case in which Pendellösung oscillations in a diffracting crystal were given rise to by linearly polarized incident X-rays having both the σ- and π-components, and pointed out that a diffracting crystal could serve as a polarizer and as a phase plate. Recently, investigations of X-ray optics using crystal polarizers and crystal phase plates were performed by Hart,[4] Annaka *et al.*,[5,6] Golovchenko *et al.*,[7] Mills,[8] Ishikawa *et al.*[9,10] and Hirano *et al.*,[11,12] which were mainly devoted to preparing circularly or elliptically polarized X-rays for magnetic scattering experiments. In the present paper, however, the author makes a proposal in which a crystal polarizer serves as 'a polarization interferometer' in X-ray topographic observations or goniometric measurements.

In observation or measurement techniques, interferometries are effective ways of giving phase informations of probing waves, which have frequently made significant progresses in physical observation and measurement techniques. In the hard X-ray frequency region of electromagnetic waves, Bonse and Hart[13–15] originally realized an interferometer of Mach-Zehnder type. The present paper proposes another feasibility of X-ray interferometry by means of interference of polarization. In the last part of the present paper, a feasibility of 'X-ray diffraction holography' is pointed out, which is however fundamentally different from so-called 'X-ray holography'[16] using soft X-rays.

§2. Methodology

2.1 *The principle of interference of polarization*

Figure 1 shows the optical system of visible light in which the x- and y-polarized lights interfere with each other. A double refractive object is located between a polarizer and an analyzer. The directions of x and y are parallel and perpendicular, respectively, to the optic axis of the object. The orientations of the polarizer and the analyzer are adjusted so as to allow the light polarized in the direction of $\boldsymbol{e}_x - \boldsymbol{e}_y$ only to pass through, $\boldsymbol{e}_x$ and $\boldsymbol{e}_y$ being the unit vectors in the directions of x and y respectively. The difference of refractive indices of the object for the x- and y-polarizations gives rise to difference in phase between the x- and y-polarized lights incident on the analyzer.

Figure 2 shows that the intensity of the light passing through the analyzer varies according to the difference in phase between the x- and y-polarized lights. In Fig. 2, D_x and D_y are corresponding to the oscillations of the x- and y-polarized lights respectively, and D_a is corresponding to the oscillation of the light passing through the analyzer. In Fig. 2(a), where there is no difference in phase between D_x and D_y,

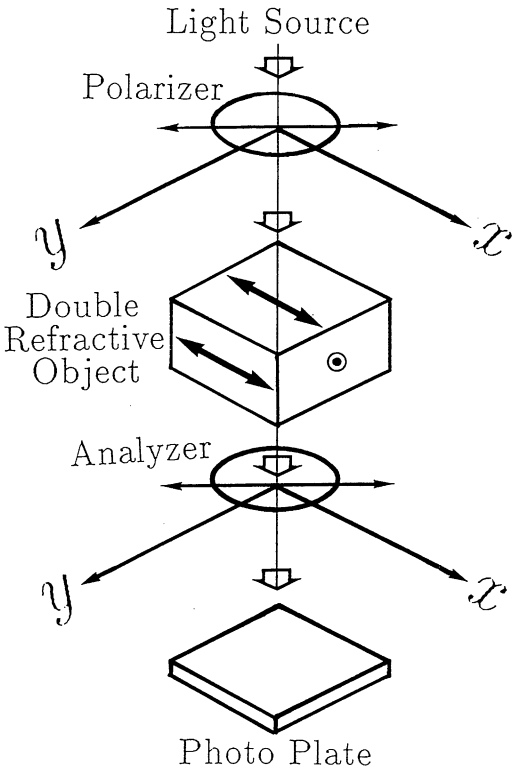

Fig. 1. A schematic diagram showing the interference of polarization. A double refractive object is located between the polarizer and the analyzer. The arrows drawn on surfaces of the object indicate the optic axis. The direction of x is parallel to the optic axis and y perpendicular to the optic axis. The difference of refractive indices gives rise to the difference of effective length of paths through which the x- and y-polarized lights pass. The intensity of the light passing through the analyzer changes due to the difference in phase between the x- and y-polarized lights as shown in Fig. 2.

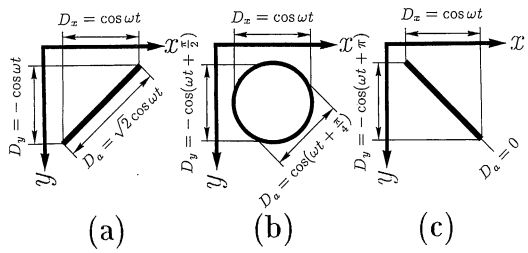

Fig. 2. Lissajous figures drawn by the x- and y-oscillations with the identical amplitude and different phases, are shown. D_x and D_y are the oscillations in the directions of x and y respectively. D_a is the oscillation projected on the line of $\boldsymbol{e}_x - \boldsymbol{e}_y$, $\boldsymbol{e}_x$ and $\boldsymbol{e}_y$ being the unit vectors in the directions of x and y respectively. D_x and D_y are corresponding to the oscillations of the x- and y-polarized lights in Fig. 1, and D_a is corresponding to the oscillation of the light passing through the analyzer in Fig. 1. The amplitude of D_a changes owing to the difference in phase between D_x and D_y.

the oscillation which D_x and D_y compose is linearly polarized in the direction of $\boldsymbol{e}_x - \boldsymbol{e}_y$, and the amplitude of D_a is $\sqrt{2}$ with the amplitudes of D_x and D_y being unities. In Fig. 2(b), where the difference in phase between D_x and D_y is $\pi/2$, the oscillation which D_x and D_y compose is circularly polarized, and the amplitude of D_a is unity. In Fig. 2(c), where the difference in phase between D_x and D_y is π, the oscillation which D_x and D_y compose is linearly polarized in the direction of $\boldsymbol{e}_x + \boldsymbol{e}_y$, and the amplitude of D_a is zero. Then, one can see that the analyzer makes the x- and y-polarized lights interfere with each other. In Fig. 1, if the beam incident on the object is a plane wave, irregularities of thickness or refractive indices of the object will be recorded on the photo plate as dark and bright contrasts.

In X-ray diffraction experiments, one can use a reflector crystal with the Bragg-reflection angle being 45 degree in place of the analyzer in Fig. 1. In the condition of the Bragg-reflection angle being 45 degree, since the direction of reflection is perpendicular to the direction of incidence, only the wave polarized perpendicularly to the plane of incidence is Bragg-reflected and the wave polarized parallelly to the plane of incidence is almost totally transmitted without being reflected. For the reflector crystal used as the analyzer, a perfect crystal of silicon is desirable. Then, in order to realize the condition of Bragg-reflection angle being 45 degree with fixed spacings of Bragg planes, the wavelength of the X-rays must be freely tunable. Therefore, the synchrotron radiation with continuous spectrum can be used effectively. Moreover, X-rays to be incident on a sample crystal with ideally linear or elliptical polarizations can be prepared relatively easily from the synchrotron radiation which is usually almost linearly polarlized. Of course, the sample crystal intended to observe in this technique of X-ray diffraction is corresponding to the double refractive object in Fig. 1. The σ- and π-polarized X-rays reflected by the sample crystal are corresponding to the

x- and y-polarized lights in Fig. 1. The method of observation may be topography or goniometry. A conceivable arrangement of topography by which informations of phases of X-rays can be obtained, will be given in the following subsection.

2.2 *A topographic technique giving phase informations of X-rays*

Figure 3 shows an optical arrangement of section topography in which phase informations of X-rays can be obtained by means of interference of polarization. In Fig. 3, the paths of the X-rays from the synchrotron radiation source to the monochromator, from the monochromator to the sample crystal, and from the sample to the analyzer crystal, are all parallel to the sheet on which the figure is drawn. The beam path from the analyzer crystal to the nuclear plate is not parallel to the sheet.

The synchrotron radiation beam monochromatized by the monochromator passes through the pinhole and is incident on the sample crystal. The beam incident on the sample crystal must consist of the beam polarized perpendicularly to the sheet (σ-polarization) and the beam polarized parallelly to the sheet (π-polarization) which have a regular ratio of amplitude and a regular relation in phase. The Bragg-reflection angle of the sample crystal must not be 45 degree. Then the beam reflected by the sample crystal has both components of the σ- and π-polarizations. In order to make the beams of the σ- and π-polarizations interfere with each other, the beam from the sample crystal is reflected by the analyzer crystal with the Bragg angle of 45 degree. The direction of the beam reflected by the analyzer crystal is not parallel or perpendicular to the sheet on which Fig. 3 is drawn. The slit is located before the nuclear plate, in order to cut off the fuzz of the image caused by the Bragg-reflection of the analyzer crystal. By moving the sample crystal in the direction perpendicular to the sheet and the nuclear plate from up to down simultaneously, a two-dimensional pattern is recorded on the nuclear plate. In the topography by this technique, the square of the absolute value of the sum of the amplitudes of the σ- and π-polarizations is obtained, in place of the sum of the intensities of the σ- and π-polarizations which is obtained by conventional section topography without analyzer crystal.

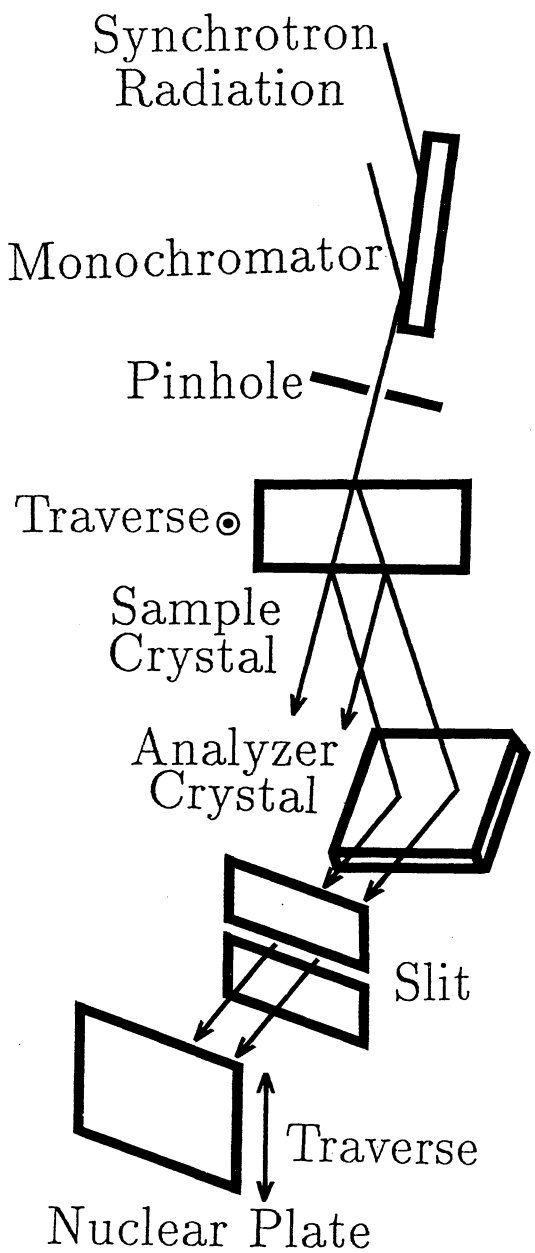

Fig. 3. A schematic drawing of the optical arrangement for the special topographic technique in which the waves of the σ- and π-polarizations reflected by the sample crystal interfere with each other being reflected by the analyzer crystal.

§3. Topographs of a Spherical Strain Field

3.1 *Experimental and simulated images in the usual topographic technique*

Figure 4 shows a section topograph of an FZ-silicon crystal obtained by using the synchrotron radiation, together with patterns numerically simulated based on the Takagi-Taupin equations.[17-20] The topograph by the experiment Fig. 4(b) was obtained using extremely high order reflection 14 14 0. The pattern was significantly disturbed by 4-fold concentric circles. The method of the simulation and the experimental techniques were given in a previous paper by the present author and co-authors.[21] The technique of the simulation was almost the same as the method given in Epelboin's reviews.[22,23] Numerically simulated patterns are in good agreement with the pattern obtained by the experiment. The strain field assumed in the simulation was spherically symmetrical and given by

$$\boldsymbol{u}=\frac{c}{r^2}\hat{\boldsymbol{r}}, \tag{1}$$

where $\boldsymbol{u}$ is the lattice displacement vector, c is the magnitude of the strain field, r is the distance from the strain source, and $\hat{\boldsymbol{r}}$ is the unit vector of the direction of r. Figure 5 shows the location of the strain source assumed in the simulations for Figs. 4(a) and 4(c). There was not significant difference between Figs. 4(a) and 4(c), for which the proportional constant c in eq. (1) was plus and minus 4×10^{-16} m^3 respectively. So, the present author could not determine the sign of the strain field although the magnitude of the strain field was estimated.

3.2 *Numerically simulated topographs by interference of polarization*

The Takagi-Taupin equations[17-19] of Kato's type[20] are given by

$$\frac{\partial D_o}{\partial s_o}=-i\pi KC\chi_{-h}\exp(-2\pi i\boldsymbol{h}\cdot\boldsymbol{u})D_h, \tag{2a}$$

$$\frac{\partial D_h}{\partial s_h}=-i\pi KC\chi_{+h}\exp(+2\pi i\boldsymbol{h}\cdot\boldsymbol{u})D_o. \tag{2b}$$

Here, D_o and D_h are the amplitudes of refracted and reflected waves, s_o and s_h are the oblique coordinates in the directions of refraction and reflection, K is the wave number of the incident wave, C is the polarization factor, $\boldsymbol{h}$ is the reflection vector, χ_{+h} and χ_{-h} are the plus and minus $\boldsymbol{h}$-th Fourier coefficients of the electric polarizability and $\boldsymbol{u}$ is the lattice displacement vector.

If the absorption of X-rays in the crystal is not taken into account, one can consider χ_{+h} and χ_{-h} to be the identical real value. When the solutions of eqs. (2a) and (2b) for a lattice displacement field $+\boldsymbol{u}$ are denoted by $D_o^{(+)}$ and $D_h^{(+)}$ and the solutions for displacement $-\boldsymbol{u}$ are $D_o^{(-)}$ and $D_h^{(-)}$, the relations of those solutions could be given apparently as follows:

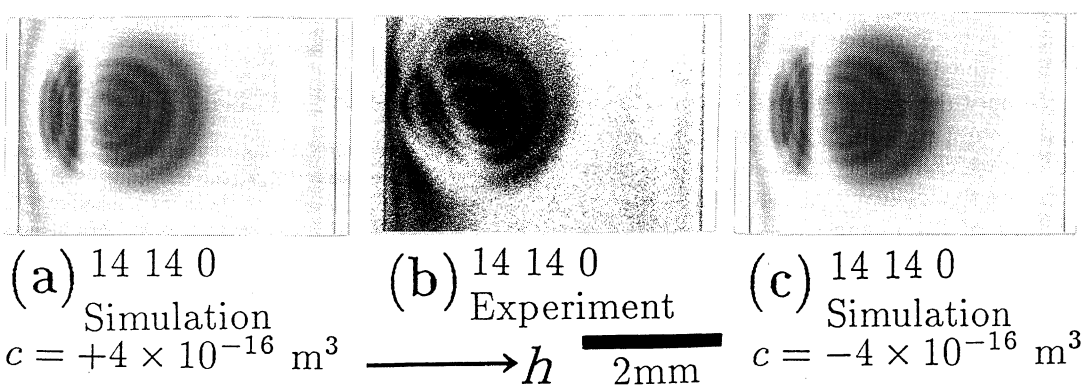

Fig. 4. The comparison between the experimental and the numerically simulated section topographs. The experiment was carried out by using the synchrotron radiation monochromatized into the wavelength 0.4 Å. The reflection index was silicon 14 14 0. The value of c indicates the magnitude of the strain field in eq. (1).

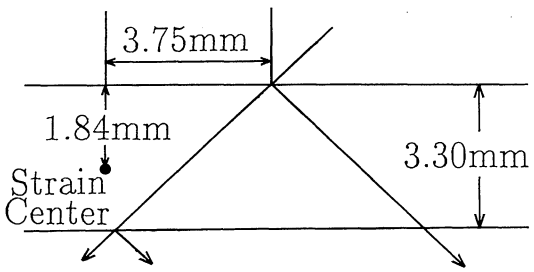

Fig. 5. The location of the strain center which was determined by the comparison between the experiment and the simulation. The big triangle is the Borrmann fan for silicon 14 14 0 reflection with the wavelength being 0.4 Å.

$$D_o^{(-)}=D_o^{(+)*}, \tag{3a}$$

$$D_h^{(-)}=-D_h^{(+)*}. \tag{3b}$$

So the absolute values of the solutions for eqs. (2a) and (2b) do not change for the reversal of the sign of the strain field. Figures 4(a) and 4(c) are slightly different because the absorption of the X-rays was taken into account in the simulation.

Further, in order to consider the solutions for two independent polarizations of the X-rays, the solutions of eqs. (2a) and (2b) for the σ- and π-polarizations will be denoted by the notations S and P respectively in place of D. We obtain the following formulae similar to eqs. (3a) and (3b).

$$S_o^{(-)}=S_o^{(+)*}, \tag{4a}$$

$$S_h^{(-)}=-S_h^{(+)*}, \tag{4b}$$

and

$$P_o^{(-)}=P_o^{(+)*}, \tag{5a}$$

$$P_h^{(-)}=-P_h^{(+)*}. \tag{5b}$$

Here, the meanings of superscripts and subscripts are the same as in eqs. (3a) and (3b). If S_h and P_h, being reflected by the analyzer crystal in Fig. 3, interfere with each other in the ratio $1:x$ with x being real, the amplitude of the wave reflected by the analyzer crystal, which will be denoted by the notation A, is given by

$$A_h^{(+)}=S_h^{(+)}+xP_h^{(+)}, \tag{6}$$

$$A_h^{(-)}=S_h^{(-)}+xP_h^{(-)}=-S_h^{(+)*}-xP_h^{(+)*} =-A_h^{(+)*}, \tag{7}$$

where the meanings of superscripts and subscripts are the same as in eqs. (3a) and (3b). Then the absolute values of $A_h^{(+)}$ and $A_h^{(-)}$ are the same. The above consideration is based on the assumption that the boundary conditions for both S_o and P_o are given by real values on the incident surface of the sample crystal, that is to say, the beam incident on the sample crystal is linearly polarized. For considering the case in which the beam incident on the sample crystal is circularly polarized, one can give the boundary condition for S_o being real and that for P_o being purely imaginary, and then estimate the interfered amplitude of the beam reflected by the analyzer crystal as S_h+xP_h with x being real. The above dealing is the same as that the boundary conditions for both S_o and P_o are real and the amplitude of the interfered wave is estimated as $S_h \pm \mathrm{i}xP_h$, because the Takagi-Taupin equations (2a) and (2b) are apparently satisfied even if the solutions D_o and D_h are multiplied by an arbitrary complex value. So, when the beam incident on the sample crystal is circularly polarized, the amplitude of the beam reflected by the analyzer crystal, which will be denoted by the notation B, is given by

$$B_h^{(+)}=S_h^{(+)}\pm \mathrm{i}xP_h^{(+)}, \tag{8}$$

$$B_h^{(-)}=S_h^{(-)}\pm \mathrm{i}xP_h^{(-)}=-S_h^{(+)*}\mp \mathrm{i}xP_h^{(+)*}, \tag{9}$$

with x being real, then in general

$$|B_h^{(+)}| \neq |B_h^{(-)}|, \tag{10}$$

where the meanings of superscripts and subscripts are the same as in eqs. (3a) and (3b) and the notations are the same as in eqs. (6) and (7). Equation (10) shows the possibility that one can determine the sign of strain field in the sample crystal by the arrangement of Fig. 3 if the beam incident on the sample is circularly polarized.

Figure 6 shows numerically simulated interference patterns, for which it was assumed that the beam incident on the sample was circularly polarized and the beams of the σ- and π-polarizations reflected by the sample interfered with each other in the ratio of 1:14. The value 14 was nearly equal to $1/\cos 2\theta_B$, θ_B being the Bragg angle of the experimental condition for Fig. 4(b). Here a spherical strain

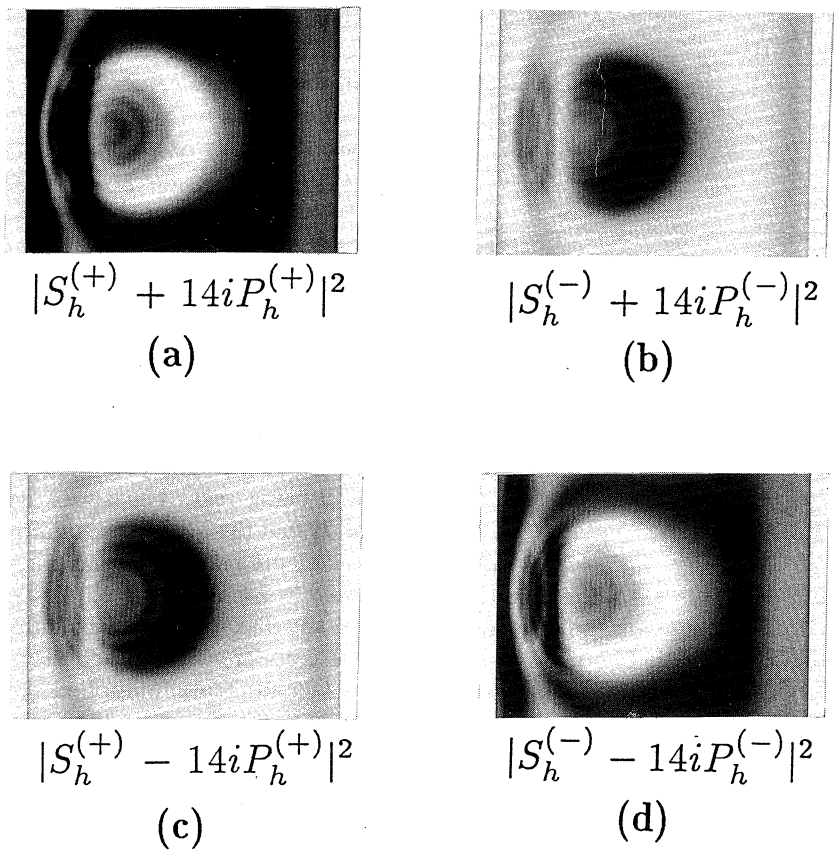

Fig. 6. Numerically simulated section topographs of the spherical strain field. These patterns were obtained on the assumption that the wave incident on the sample crystal was circularly polarized and the waves of the σ- and π-polarizations reflected by the sample crystal interfered with each other.

field was assumed in the same way as for Figs. 4(a) and 4(c). One can see the reversal of the contrasts owing to the change of sign of the strain field and the opposite rotation of the circular polarization of the beam incident on the sample crystal.

§4. A Feasibility of X-Ray Diffraction Holography

If in Fig. 1 the wavefront of the light of the x-polarization only is deformed by irregularities of the object and the light of the y-polarization is not modulated by the object, the firsthand information of the phase of the x-polarized light will be recorded on the photo plate. This is nothing but the hologram which was made by the interference of the x-polarized light and the y-polarized light which are corresponding to the object wave and the reference wave respectively.

The condition mentioned above can be realized in X-ray diffraction. When regularly polarized plane wave X-rays incident on the sample crystal satisfy the diffraction condition with the Bragg-reflection angle being 45 degree, the transmitted wave of the σ-polarization is modulated by the crystal imperfections but the transmitted wave of the π-polarization passes through the sample crystal without being Bragg-reflected. When the transmitted waves of the σ- and π-polarizations interfere with each other in the way described in previous sections, an X-ray diffraction holography is realized where the σ-polarized wave is corresponding to the object wave and the π-polarized wave is the reference wave. Generally in holography, the wave emitted from the source must be highly coherent because the wave is

split into two waves propagating in the different paths, that is, the reference wave and the object wave. In the X-ray diffraction holography described above, however, the coherence length of the plane wave X-rays in the direction of transmission have to be not so long because the reference wave and the object wave pass through the identical path in the sample crystal.

§5. Summary

In this paper, the present author proposed a method of X-ray diffraction in which informations of phases of X-rays could be obtained. It was shown by numerical simulations based on the Takagi-Taupin equations that the sign of a spherical strain field could be determined by a special technique of topography, in which a beam incident on the sample was circularly polarized and Bragg-reflected σ- and π-polarized X-rays interfered with each other being reflected by the analyzer crystal. Moreover, a feasibility of X-ray diffraction holography by the same principle was pointed out.

References

1) H. Hattori, H. Kuriyama and N. Kato: J. Phys. Soc. Jpn. **20** (1965) 1047.
2) M. Hart and A. R. Lang: Acta Crystallogr. **19** (1965) 73.
3) P. Skalicky and C. Malgrange: Acta Crystallogr. A**28** (1972) 501.
4) M. Hart: Philos. Mag. B**38** (1978) 41.
5) S. Annaka, T. Suzuki and K. Onoue: Acta Crystallogr. A**36** (1980) 151.
6) S. Annaka: J. Phys. Soc. Jpn. **51** (1982) 1927.
7) J. A. Golovchenko, B. M. Kincaid, R. A. Levesque, A. E. Meixner and D. R. Kaplan: Phys. Rev. Lett. **57** (1986) 202.
8) D. M. Mills: Phys. Rev. B**36** (1987) 6178.
9) T. Ishikawa, K. Hirano and S. Kikuta: J. Appl. Crystallogr. **24** (1991) 982.
10) T. Ishikawa, K. Hirano, K. Kanzaki and S. Kikuta: Rev. Sci. Instrum. **63** (1992) 1098.
11) K. Hirano, K. Izumi, T. Ishikawa, S. Annaka and S. Kikuta: Jpn. J. Appl. Phys. **30** (1991) L407.
12) K. Hirano, K. Kanzaki, M. Mikami, M. Miura, K. Tamasaku, T. Ishikawa and S. Kikuta: J. Appl. Crystallogr. **25** (1992) 531.
13) U. Bonse and M. Hart: Appl. Phys. Lett. **6** (1965) 155.
14) U. Bonse and M. Hart: Appl. Phys. Lett. **7** (1965) 99.
15) U. Bonse and M. Hart: Appl. Phys. Lett. **7** (1965) 239.
16) For example, M. R. Howells and C. J. Jacobsen: Synchrotron Radiation News **3** (1990) 23.
17) S. Takagi: Acta Crystallogr. **15** (1962) 1311.
18) S. Takagi: J. Phys. Soc. Jpn. **26** (1969) 1239.
19) D. Taupin: Bull. Soc. Fr. Min. Crist. **87** (1964) 469.
20) N. Kato: Z. Naturforsch. a **28** (1973) 604.
21) K. Okitsu, S. Iida, Y. Sugita, H. Takeno, Y. Yagou and H. Kawata: Jpn. J. Appl. Phys. **31** (1992) 3779.
22) Y. Epelboin: Mater. Sci. Engng. **73** (1985) 1.
23) Y. Epelboin: Prog. Cryst. Growth Charact. **14** (1987) 465.